crystallization communications

Crystallization and preliminary X-ray characterization of the *glpX*-encoded class II fructose-1,6-bisphosphatase from *Mycobacterium tuberculosis*

Hiten J. Gutka,[a,b,c] Scott G. Franzblau,[a,b] Farahnaz Movahedzadeh[a,b]* and Cele Abad-Zapatero[b,c]*

[a]Institute for Tuberculosis Research, University of Illinois at Chicago, Chicago, IL 60607, USA, [b]Department of Medicinal Chemistry and Pharmacognosy, University of Illinois at Chicago, Chicago, IL 60607, USA, and [c]Center for Pharmaceutical Biotechnology, University of Illinois at Chicago, Chicago, IL 60607, USA

Correspondence e-mail: movahed@uic.edu, caz@uic.edu

Fructose-1,6-bisphosphatase (FBPase; EC 3.1.3.11), which is a key enzyme in gluconeogenesis, catalyzes the hydrolysis of fructose 1,6-bisphosphate to form fructose 6-phosphate and orthophosphate. The present investigation reports the crystallization and preliminary crystallographic studies of the *glpX*-encoded class II FBPase from *Mycobacterium tuberculosis* H37Rv. The recombinant protein, which was cloned using an *Escherichia coli* expression system, was purified and crystallized using the hanging-drop vapor-diffusion method. The crystals diffracted to a resolution of 2.7 Å and belonged to the hexagonal space group $P6_122$, with unit-cell parameters $a = b = 131.3$, $c = 143.2$ Å. The structure has been solved by molecular replacement and is currently undergoing refinement.

1. Introduction

Mycobacterium tuberculosis (*Mtb*), which infects about one-third of the human population, is the leading cause of mortality arising from bacterial pathogens. In 2006, over nine million new cases and 1.7 million deaths occurred owing to TB (World Health Organization, 2008). Tuberculosis is a worldwide health threat in conjunction with the spread of HIV infection (Nunn *et al.*, 2005). The pathogen is capable of surviving and replicating in the host macrophage, which is an important factor in the persistence of the disease.

Enzymatic pathways that are involved in growth and survival under nutritionally restrictive and stressful conditions *in vivo* represent attractive alternative targets for the development of novel antimicrobial agents. Although *Mtb* is capable of growth on a variety of substrates *in vitro*, there is evidence that suggests that during infection *Mtb* preferentially utilizes fatty acids as a source of energy (Boshoff & Barry, 2005). Moreover, genes involved in fatty-acid utilization (glyoxylate shunt, *icl*; gluconeogenesis, *glpX* and *pckA*) are required for growth and persistence *in vivo* (Sharma *et al.*, 2000; Collins *et al.*, 2002; Liu *et al.*, 2003; Sassetti & Rubin, 2003; Muñoz-Elías & McKinney, 2005; Dunn *et al.*, 2009; Marrero *et al.*, 2010). Hence, the enzymes that catalyze the glyoxylate shunt and gluconeogenesis pathways are considered to be potential targets for the discovery of new drugs (Sharma *et al.*, 2000; Smith *et al.*, 2003; Anstrom & Remington, 2006; Purohit *et al.*, 2007). A recent study (Marrero *et al.*, 2010) demonstrated that phosphoenolpyruvate carboxykinase (PEPCK; EC 4.1.1.32) plays a pivotal role in the pathogenesis of *Mtb*. PEPCK is the enzyme encoded by *pckA* and connects the TCA cycle and gluconeogenesis by catalyzing the reversible decarboxylation and phosphorylation of oxaloacetate (OAA) to form phosphoenolpyruvate (PEP).

Furthermore, it has also been shown that PEPCK is essential for the growth and survival of *Mtb* during infection in mice, wherein the pathogen relies primarily on gluconeogenic substrates for *in vivo* growth and persistence (Marrero *et al.*, 2010). Recently, efforts have been directed towards solving the three-dimensional structure of PEPCK in order to enhance our understanding of this important enzyme (Chim *et al.*, 2011). Apart from these recent studies, the role of gluconeogenesis in *Mtb* pathogenesis remains largely unexplored. Therefore, understanding the key enzymes of the gluconeogenic pathway and obtaining key structural information about the enzymes involved in gluconeogenesis becomes important.

Fructose-1,6-bisphosphatase (FBPase; EC 3.1.3.11), a key enzyme in gluconeogenesis, catalyzes the hydrolysis of fructose 1,6-bisphosphate to form fructose 6-phosphate and orthophosphate. In glycolysis, the opposite reaction is catalyzed by phosphofructokinase whose product is fructose 6-phosphate, an important precursor in various biosynthetic pathways (Pontremoli *et al.*, 1975). FBPases are members of the large superfamily of lithium-sensitive phosphatases, which includes both the inositol phosphatases and FBPases.

Five different classes (or types) of FBPases have been identified based on their amino-acid sequences (FBPases I–V; Donahue *et al.*, 2000; Nishimasu *et al.*, 2004; Hines *et al.*, 2006). Although the class I FBPases are most widely distributed among living organisms, many microorganisms such as *Escherichia coli* possess both class I and class II FBPases. The structural biology and the underlying regulatory mechanism of class I FBPases have been extensively studied and are well understood (Hines *et al.*, 2006; Hines, Fromm *et al.*, 2007; Hines, Kruesel *et al.*, 2007).

The type II FBPase in *E. coli* is encoded by the *glpX* gene, which is part of the glycerol 3-phosphate regulon (Donahue *et al.*, 2000).

Crystal structures of this enzyme have recently been reported in both the apo form and with substrate and catalytic products (PDB entries 3bih, 3big and 3d1r; Brown *et al.*, 2009). In addition, structures of the same enzyme, previously referred to as 'glycerol metabolism protein', from *E. coli* are also available in the PDB (PDB entries 1ni9 and 2r8t; Brown *et al.*, 2009; V. V. Lunin, T. Skarina, G. Brown, R. Sanishvili, A. Yakunin, A. Joachimiak, A. M. Edwards & A. Savchenko, unpublished work).

Initial genome sequencing and annotation of *Mtb* revealed the absence of a class I FBPase homolog (Cole *et al.*, 1998). Later, results of genetic and biochemical analyses revealed that the *Rv1099c* gene of *Mtb* encodes the missing mycobacterial class II FBPase (Movahedzadeh *et al.*, 2004). The protein encoded by the *Mtb glpX* (*Rv1099c*) gene has been shown experimentally to possess FBPase activity and is homologous to other experimentally verified class II FBPases from *E. coli* (GlpX; 42% identity) and *Corynebacterium glutamicum* (65% identity; Rittmann *et al.*, 2003). Since the *Mtb* FBPase II has no human homolog, biochemical and structural studies may reveal certain characteristics that are unique to *Mtb* FBPase II and that may possibly be exploited for species-specific drug discovery targeting this enzyme. We have recently reported the cloning, expression, purification and initial biochemical characterization of the recombinant mycobacterial class II FBPase (Gutka *et al.*, 2011). The crystallization, preliminary X-ray diffraction analysis and initial results of the structure determination of this enzyme are presented here.

2. Materials and methods

2.1. Expression and purification of *Mtb* FBPase

Unless mentioned otherwise, all reagents and chemicals were purchased from Fisher Scientific, Pittsburgh, Pennsylvania, USA. The *glpX* gene (*Rv1099c*) encoding the class II FBPase from *Mtb* H37Rv was PCR-amplified using gene-specific primers and cloned into the pET15b vector as described previously (Gutka *et al.*, 2011). The expression and purification process followed was the same as that described elsewhere (Gutka *et al.*, 2011). Briefly, *E. coli* BL21 (DE3) harboring pET15b-FBPase was grown at 310 K in 4 l LB broth containing 100 µg ml^{-1} ampicillin until the OD_{600} was about 0.5 and was then induced with isopropyl β-D-1-thiogalactopyranoside (IPTG) at a final concentration of 0.5 mM. The culture was grown for a further 8 h at 298 K and then centrifuged at 4000g for 20 min at 277 K. The cells

were washed with phosphate-buffered saline and stored at 250 K until further use. The cell pellets collected from the 4 l culture were gently stirred at 277 K for 45 min with the addition of buffer A (50 mM sodium phosphate buffer pH 8.0 and 300 mM NaCl), 0.50 mg ml^{-1} lysozyme, 2 U ml^{-1} DNAse I (Sigma–Aldrich, St Louis, Missouri, USA) and Complete EDTA-free protease inhibitor (Roche Molecular Biochemicals, Indianapolis, Indiana, USA). The lysed cell pellet was subjected to sonication on ice for a total time of 20 min following a fixed sonication–lysis protocol. Insoluble cell debris was removed by centrifugation at 16 000g for 30 min at 277 K. The supernatant was filter-clarified through a 0.45 µm PVDF syringe filter (Millipore, Billerica, Massachusetts, USA) and loaded onto Ni–NTA Bind Resin (Novagen, Gibbstown, New Jersey, USA) pre-equilibrated in buffer A (50 mM sodium phosphate buffer pH 8.0 and 300 mM NaCl) with 10 mM imidazole. *Mtb* FBPase bound to the Ni–NTA column, which was then washed with 32 column volumes of buffer A plus 20 mM imidazole followed by 40 column volumes of buffer A plus 50 mM imidazole. *Mtb* FBPase was eluted from the column with six column volumes of buffer A plus 250 mM imidazole. The eluate was immediately subjected to buffer exchange and concentration in an Amicon-15 Ultracel 100K (Millipore, Billerica, Massachusetts, USA) centrifuge concentrator against exchange buffer [20 mM tricine, 50 mM KCl, 1 mM MgCl$_2$, 0.1 mM DTT, 15%(v/v) glycerol pH 7.7] prior to size-exclusion chromatography as described for FBPase II from *C. glutamicum* (Rittmann *et al.*, 2003). *Mtb* FBPase was applied onto a Superdex 200 HiLoad 26/60 column (GE Healthcare Biosciences, Piscataway, New Jersey, USA) on an ÄKTApurifier system (GE Healthcare Biosciences, Piscataway, New Jersey, USA) pre-equilibrated with exchange buffer and eluted at a low flow rate of 1 ml min^{-1}. 3 ml fractions were collected and were pooled according to the chromatogram and the observed purity profile on SDS–PAGE. The pooled fractions were concentrated and filtered through a 0.22 µm membrane filter. For analytical purposes, equal volumes of samples from different purification stages were analyzed by SDS–PAGE. All protein-purification steps were performed at 277 K. The protein concentration was estimated using the Bradford method (Bradford, 1976).

2.2. Crystallization

For crystallization, purified His-tagged recombinant *Mtb* FBPase was concentrated to 10 mg ml^{-1} in exchange buffer. Crystallization trials were performed by the hanging-drop vapor-diffusion method and suitable crystallization conditions were found from Index Screens I and II (Hampton Research, Aliso Viejo, California, USA). The crystals grew in the temperature range 295–300 K. Crystals were obtained by mixing 1 µl protein solution with 1 µl reservoir solution consisting of 1.8 M ammonium citrate tribasic pH 7.0. The volume of the reservoir solution was 300 µl per well.

2.3. Data collection and processing

The crystals were soaked in a cryoprotectant consisting of the reservoir solution (1.8 M ammonium citrate tribasic pH 7.0) plus 20%(v/v) glycerol. Subsequently, the crystals were flash-frozen in liquid nitrogen at 100 K. X-ray diffraction data for *Mtb* FBPase were collected from a single frozen crystal using a MAR 300 CCD detector on the Southeast Regional Collaborative Access Team (SER-CAT) 22-ID beamline at the Advanced Photon Source, Argonne National Laboratory, Illinois, USA. A total of 360 frames were collected with 1° scan width and 1 s exposure time. The crystal-to-detector distance was set to 280 mm. The data were indexed and scaled with the *HKL*-2000 package (Otwinowski & Minor, 1997).

crystallization communications

3. Results and discussion

The recombinant His-tagged FBPase was purified to homogeneity from the soluble fraction by a combination of Ni–NTA and size-exclusion chromatography. The N-terminal hexahistidine tag was not removed from the protein. The Ni–NTA eluate was relatively impure, with some low-molecular-weight and high-molecular-weight impurities; hence, an additional step of size-exclusion chromatography was introduced to purify the protein to homogeneity (Gutka *et al.*, 2011). Fractions 18–20 from the size-exclusion column were the most pure and had high protein content (Fig. 1*a*); thus, they were pooled for further studies. The final purified *Mtb* FBPase protein appeared as a single band of approximately 37 kDa on SDS–PAGE (Fig. 1, fractions 15–22).

Many hexagonal-looking crystals (Fig. 2) were found after 72 h using 1.8 *M* ammonium citrate tribasic pH 7.0 as the reservoir solution. The crystals grew to full size in about two weeks. Larger crystals were easily obtained by increasing the total drop volume to 4 µl (2 µl each of protein solution and precipitating agent) and 6 µl (3 µl each of protein solution and precipitating agent), indicating that the crystallization condition is scalable. The presence of *Mtb* FBPase protein in these crystals was confirmed by running an SDS–PAGE gel after dissolving these crystals in the gel-loading buffer.
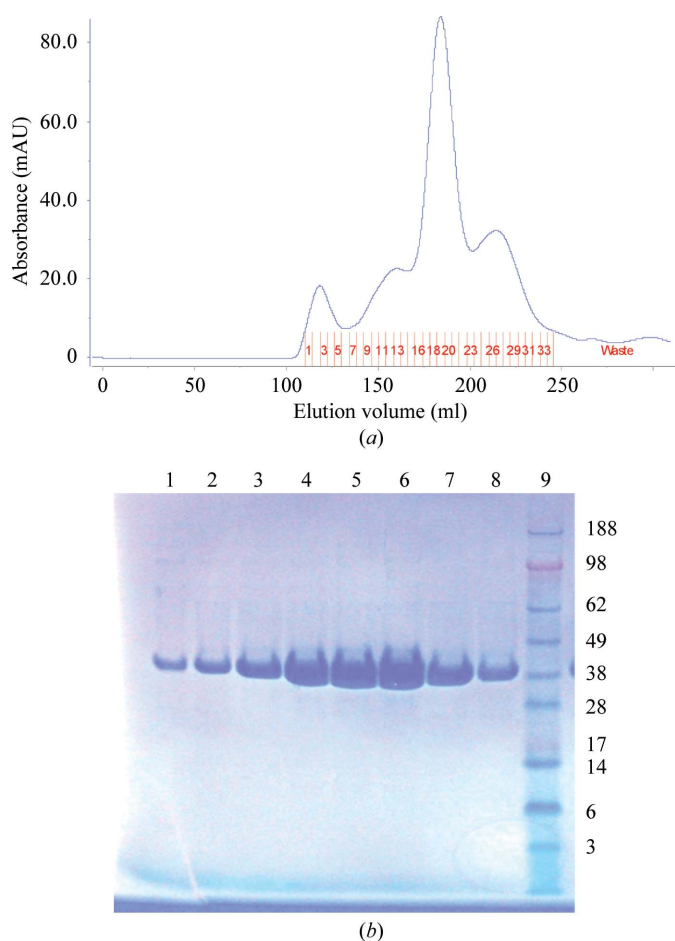
Diffraction data were collected using a single crystal cryoprotected with 1.8 *M* ammonium citrate tribasic pH 7.0 plus 20%(v/v) glycerol. The crystal diffracted to 2.7 Å resolution and a data set with an overall completeness of 98.5% was collected. Symmetry and systematically absent reflections suggested that the *Mtb* FBPase crystals belonged to space group $P6_122$ (or its enantiomer $P6_522$),
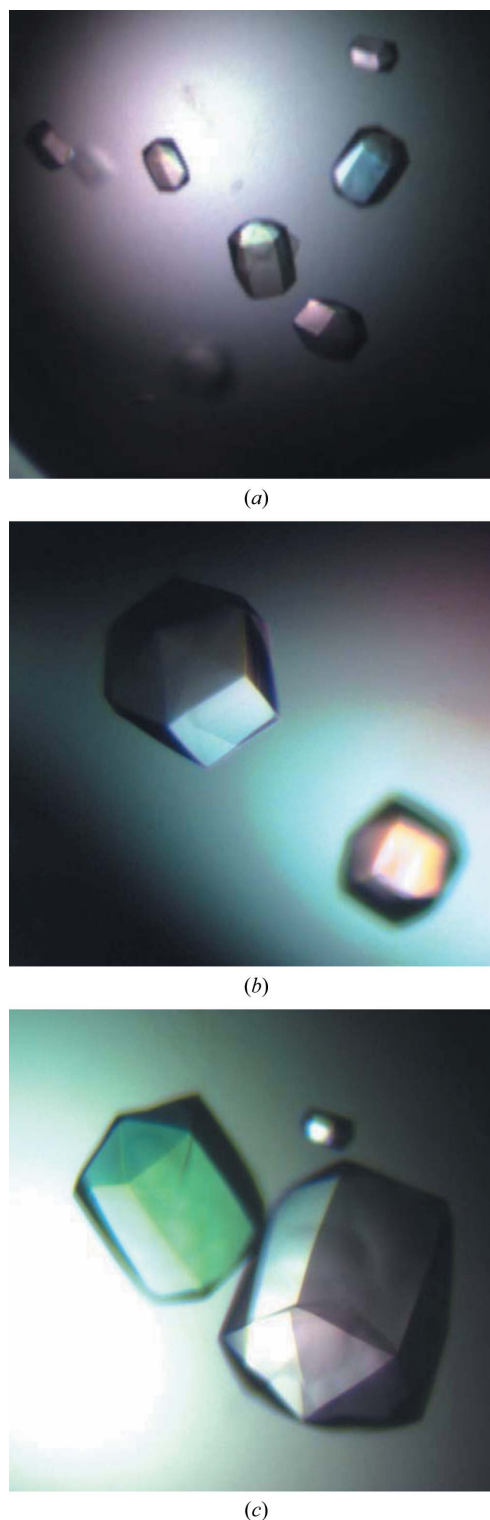

(*a*)

(*b*)

(*c*)

Figure 2
(*a*) Hexagonal crystals of *Mtb* FBPase obtained at pH 7.0. (*b*, *c*) Larger crystals of *Mtb* FBPase obtained under similar conditions with increased drop volumes.

(*a*)

(*b*)

Figure 1
(*a*) Size-exclusion profile of the affinity-captured protein showing several low-molecular-weight and high-molecular-weight impurities in addition to the main peak of *Mtb* FBPase. Only the fractions (18–20) corresponding to the main peak were used in the crystallization experiments. (*b*) Lanes 1–8, SDS–PAGE profile of SEC fractions 15–22. Lane 9, SeeBlue Plus2 molecular-weight standards (labeled in kDa).

Table 1
Data-collection and processing statistics.

Values in parentheses are for the last shell.

Synchrotron-radiation source	22-ID, SER-CAT, APS
Wavelength (Å)	1.0000
Space group	$P6_122$
Unit-cell parameters (Å)	$a = b = 131.3$, $c = 143.2$
Total No. of reflections	212726
No. of unique reflections	20561
Multiplicity	10.4 (7.2)
Resolution (Å)	40–2.7 (2.75–2.70)
Completeness (%)	98.5 (88.1)
R_{merge}†	0.092 (0.686)
$\langle I/\sigma(I)\rangle$	5.3 (2.0)
Mosaicity (°)	0.43
Wilson plot (B overall) (Å^2)	71.5

† $R_{merge} = \sum_{hkl} \sum_i |I_i(hkl) - \langle I(hkl)\rangle| / \sum_{hkl} \sum_i I_i(hkl)$.

with unit-cell parameters $a = b = 131.3$, $c = 143.2$ Å, even though the weak reflections in the higher resolution shells had a high R_{merge} (Table 1) which could indicate a lower symmetry space group. The cross-rotation function was calculated using the program *Phaser* from the *CCP*4 suite (Winn *et al.*, 2011).

Determination of the Matthews coefficient suggested the presence of 50.3% solvent content in the unit cell ($V_M = 2.47$ Å^3 Da^{-1}) with a dimer in the asymmetric unit of the higher symmetry space group (Matthews, 1968). The data-collection statistics are shown in Table 1.

Initially, the possibility of the space group being $P6_1$ could not be excluded. Thus, an initial search was undertaken using the *Phaser* program (McCoy *et al.*, 2007) from the *CCP*4 suite (Winn *et al.*, 2011) using the *E. coli* GlpX monomer as a probe (PDB entry 3d1r; Brown *et al.*, 2009) in space group $P6_1$ and looking for four monomers in the asymmetric unit. No complete solution was found; however, a reproducible dimer was recognized among the partial solutions. This dimer differed from that suggested previously as a functional unit for the *E. coli* enzyme (Brown *et al.*, 2009) and was used as a search model in space group $P6_122$. A solution was found with *MOLREP* as implemented in the *CCP*4 suite (Winn *et al.*, 2011). The crystallographic statistics for $P6_122$ with one dimer in the asymmetric unit were an R factor of 0.504 and a correlation coefficient of 0.574; those for $P6_522$ were an R factor of 0.632 and a correlation coefficient of 0.308, indicating $P6_122$ to be the correct solution.

This preliminary model allowed the construction of a revised *Mtb* FBPase model with the correct sequence and initial refinement (using *REFMAC* as implemented in the *Coot* software) proceeded normally [$R_{free} = 0.390$, R value (working + test) = 0.332 and R value (working) = 0.329; Murshudov *et al.*, 2011]. Further refinement of this structure is in progress and the final structural results will be reported in due course.

References

Anstrom, D. M. & Remington, S. J. (2006). *Protein Sci.* **15**, 2002–2007.
Boshoff, H. I. & Barry, C. E. III (2005). *Nature Rev. Microbiol.* **3**, 70–80.
Bradford, M. M. (1976). *Anal. Biochem.* **72**, 248–254.
Brown, G., Singer, A., Lunin, V. V., Proudfoot, M., Skarina, T., Flick, R., Kochinyan, S., Sanishvili, R., Joachimiak, A., Edwards, A. M., Savchenko, A. & Yakunin, A. F. (2009). *J. Biol. Chem.* **284**, 3784–3792.
Chim, N. *et al.* (2011). *Tuberculosis*, **91**, 155–172.
Cole, S. T. *et al.* (1998). *Nature (London)*, **393**, 537–544.
Collins, D. M., Wilson, T., Campbell, S., Buddle, B. M., Wards, B. J., Hotter, G. & De Lisle, G. W. (2002). *Microbiology*, **148**, 3019–3027.
Donahue, J. L., Bownas, J. L., Niehaus, W. G. & Larson, T. J. (2000). *J. Bacteriol.* **182**, 5624–5627.
Dunn, M. F., Ramírez-Trujillo, J. A. & Hernández-Lucas, I. (2009). *Microbiology*, **155**, 3166–3175.
Gutka, H. J., Rukseree, K., Wheeler, P. R., Franzblau, S. G. & Movahedzadeh, F. (2011). *Appl. Biochem. Biotechnol.*, doi:10.1007/s12010-011-9219-x.
Hines, J. K., Fromm, H. J. & Honzatko, R. B. (2006). *J. Biol. Chem.* **281**, 18386–18393.
Hines, J. K., Fromm, H. J. & Honzatko, R. B. (2007). *J. Biol. Chem.* **282**, 11696–11704.
Hines, J. K., Kruesel, C. E., Fromm, H. J. & Honzatko, R. B. (2007). *J. Biol. Chem.* **282**, 24697–24706.
Liu, K., Yu, J. & Russell, D. G. (2003). *Microbiology*, **149**, 1829–1835.
Marrero, J., Rhee, K. Y., Schnappinger, D., Pethe, K. & Ehrt, S. (2010). *Proc. Natl Acad. Sci. USA*, **107**, 9819–9824.
Matthews, B. W. (1968). *J. Mol. Biol.* **33**, 491–497.
McCoy, A. J., Grosse-Kunstleve, R. W., Adams, P. D., Winn, M. D., Storoni, L. C. & Read, R. J. (2007). *J. Appl. Cryst.* **40**, 658–674.
Movahedzadeh, F., Rison, S. C., Wheeler, P. R., Kendall, S. L., Larson, T. J. & Stoker, N. G. (2004). *Microbiology*, **150**, 3499–3505.
Muñoz-Elías, E. J. & McKinney, J. D. (2005). *Nature Med.* **11**, 638–644.
Murshudov, G. N., Skubák, P., Lebedev, A. A., Pannu, N. S., Steiner, R. A., Nicholls, R. A., Winn, M. D., Long, F. & Vagin, A. A. (2011). *Acta Cryst.* D**67**, 355–367.
Nishimasu, H., Fushinobu, S., Shoun, H. & Wakagi, T. (2004). *Structure*, **12**, 949–959.
Nunn, P., Williams, B., Floyd, K., Dye, C., Elzinga, G. & Raviglione, M. (2005). *Nature Rev. Immunol.* **5**, 819–826.
Otwinowski, Z. & Minor, W. (1997). *Methods Enzymol.* **276**, 307–326.
Pontremoli, S., De Flora, A., Salamino, F., Melloni, E. & Horecker, B. L. (1975). *Proc. Natl Acad. Sci. USA*, **72**, 2969–2973.
Purohit, H. J., Cheema, S., Lal, S., Raut, C. P. & Kalia, V. C. (2007). *Infect. Disord. Drug Targets*, **7**, 245–250.
Rittmann, D., Schaffer, S., Wendisch, V. F. & Sahm, H. (2003). *Arch. Microbiol.* **180**, 285–292.
Sassetti, C. M. & Rubin, E. J. (2003). *Proc. Natl Acad. Sci. USA*, **100**, 12989–12994.
Sharma, V., Sharma, S., Hoener zu Bentrup, K., McKinney, J. D., Russell, D. G., Jacobs, W. R. & Sacchettini, J. C. (2000). *Nature Struct. Biol.* **7**, 663–668.
Smith, C. V., Huang, C., Miczak, A., Russell, D. G., Sacchettini, J. C. & Höner zu Bentrup, K. (2003). *J. Biol. Chem.* **278**, 1735–1743.
Winn, M. D. *et al.* (2011). *Acta Cryst.* D**67**, 235–242.
World Health Organization (2008). *Global Tuberculosis Control: Surveillance, Planning, Financing.* WHO Report WHO/HTM/TB/2008.393. Geneva: World Health Organization.